Bulletin of Engineering Geology and the Environment (2023) 82:135
https://doi.org/10.1007/s10064-023-03167-7

ORIGINAL PAPER

Quantifying the particle shape and surface roughness of sands

Ting Yao[1,2] · **Wei Li**[3]

Received: 7 November 2022 / Accepted: 7 March 2023 / Published online: 23 March 2023

Abstract
Particle shape and surface roughness affect both the macro- and micro-mechanical behaviour of natural sands. In geotechnical practice, the global shape of sands is generally characterized by visual comparison to reference charts or by static image analysis with a limited number of particles. Meanwhile, due to the difficulty in measuring surface roughness of sand grains, it is usually ignored in the quantification of particle morphology. In this study, the global shape of four types of natural sand, Leighton Buzzard sand (LBS), beach sand (BS), carbonate sand (CS), and completely decomposed granite soil (CDG), was measured by a dynamic particle shape analyser, and quantified using three parameters, i.e., aspect ratio, sphericity and convexity. The influence of mineralogy, depositional environment, and particle size on the global shape has been thoroughly discussed. Among the four sands, the shape descriptors of LBS are the highest, indicating the most spherical and rounded shape, because of the aqueous traction transportation. The sphericity of CDG increases with decreasing particle size due to the abrasion or collapsing of asperities of coarser particles under subsequent weathering. The surface roughness of LBS, BS and CS was successfully measured by an optical interferometer, and quantitatively characterized by the flattened root-mean square roughness (RMS_f). The RMS_f of particles with different mineralogy and sizes all tends to be stable at relatively larger size of field of view. Among the tested granular materials, the surface of CS particles is the roughest and most variable, and the finer the CS particles, the rougher the surfaces.

Keywords Particle shape · Surface roughness · Particle size · Mineralogy · Depositional environment

Introduction

Natural sands are made of discrete particles with a variety of shapes. A large number of experimental studies have shown that particle shape significantly affects the void ratio, compressibility, internal friction angle, and small-strain stiffness of granular soil (Cho et al. 2006; Dyskin et al. 2001; Otsubo et al. 2015; Li and Coop 2019). The sand particle's shape also affects the inter-particle friction coefficient (e.g., Sandeep et al. 2017; Nardelli and Coop 2019) and contact behaviour (Cavarretta et al. 2010; Yao et al. 2021) at particle scale. Therefore, quantifying particle shape is of significant importance for a comprehensive understanding of the soil mechanical behaviour (Alshibli and Alsaleh 2004; Cho et al. 2006; Li et al. 2018). Particle shape is generally characterized at three orders: form, roundness, and surface roughness as proposed by Barrett (1980) and Blott and Pye (2008). Form (global shape) represents the overall shape of sand particles at macro-scale and is generally quantified by sphericity, which is a measure of the degree of conformity of particle shape to that of a sphere (Alshibli and Alsaleh 2004), roundness reflects the angularity of the corners at meso-scale, and surface roughness (smooth or rough) accounts for the surface texture of sand particles at micro-scale (Mitchell and Soga 2005).

Digital image analysis method is gaining popularity in the quantification of both two-dimensional (2D) and three-dimensional (3D) particle shape. The static image analyses, e.g., scanning electron microscopy (SEM) (Li et al. 2018), X-ray micro-computed tomography (μCT) (Zhou et al. 2020), and 3D laser scanning (Yao et al. 2022), can quantify the shape of non-moving particles. However, the small sample size results

✉ Wei Li
liwei890508@126.com

[1] Sate Key Laboratory of Geomechanics and Geotechnical Engineering, Institute of Rock and Soil Mechanics, Chinese Academy of Sciences, Wuhan, People's Republic of China

[2] Key Laboratory of Special Environment Road Engineering of Hunan Province, Changsha University of Science & Technology, Changsha, Hunan, People's Republic of China

[3] Faculty of Engineering, China University of Geosciences, Wuhan, People's Republic of China

in low statistical relevance of data (Altuhafi et al. 2013; Wei et al. 2020), and hinders their routine use in the particle shape characterization. In contrast, the dynamic image analysis, which images a flow of moving particles, e.g., QicPic (Sympatec GmbH, Clausthal-Zellerfeld, Germany) and PartAn^{3D} (Microtrac Inc., US) particle shape analysers, can obtain the particle projections at arbitrary direction and the sample size can be significantly enlarged (Witt et al. 2004). Hence, it could acquire a more reliable statistical result by measuring a much larger quantity of particles than static image analysis method. This method has been successfully adopted to quantify the particle shape of granular soil with size from 0.063 to 35 mm (Altuhafi et al. 2013; Yao et al. 2019; Wei et al. 2020).

Because of the practical difficulty in measuring surface roughness, it is usually ignored in the description of particle shape and occasionally described qualitatively by SEM image (Santamarina and Cascante 1998). However, both experimental studies and discrete element method (DEM) modelling show that the surface roughness has a significant effect on shear modulus and inter-particle friction angle of granular soils (Santamarina and Cascante 1998; Yimsiri and Soga 2000; Li and Kim 2008; Otsubo and O'Sullivan 2018). In those experimental studies, the tested materials are artificially manufactured, such as steel balls and glass beads having uniform surface properties. So far, the study on the quantitative description of surface roughness of natural soil grains remains limited (Alshibli and Alsaleh 2004; Yang et al. 2016; Yao et al. 2019).

In the current work, with the help of a dynamic particle shape analyser (QicPic), the particle shape of four types of natural sands with different sizes, i.e., Leighton Buzzard sand (LBS), beach sand (BS), carbonate sand (CS), and completely decomposed granite soil (CDG), was quantified by three shape descriptors. The influence of mineralogy, depositional environment, and particle size on the global shape of sand was discussed. Optical interferometry which enables the surface roughness measurement of soil grains was successfully applied on two quartz sands (LBS and BS) and a carbonate sand (CS). The roughness was quantified by the flattened root-mean-square surface roughness (RMS_f), and the effect of the size of the field of view on the quantification of RMS_f was discussed. Finally, the RMS_f values of sand grains with different mineral compositions and sizes were compared to investigate their effects on natural soil surface roughness.

Materials and apparatus

Tested materials

In this study, four kinds of natural sand, LBS, BS, CS, and CDG, with sizes ranging from 0.063 mm to 2.36 mm were tested. All sands were oven-dried and sieved following the British Standards BS1377-2 (2022) prior to test, and their particle size distributions were shown in Fig. 1. For BS, the number of particles finer than 1.18 mm is quite limited, as they are more likely to be washed away from the coast. Figure 2 shows the SEM images (Hitachi S3400N VP scanning electron microscope) and energy-dispersive X-ray spectroscopy (EDX) results of LBS, BS, CDG and CS with grain size of 1.18–2.0 mm. The SEM apparatus adopted is a high performance, user-friendly with unique VP-mode that allows microscopy of samples in their natural state without the need of conventional sample preparation (coating).

The LBS is a kind of fluvial deposit, and made up of almost pure quartz as the proportion of SiO_2 is more than 80% (Fig. 2a). It is usually used as a standard sand in geotechnical engineering lab tests in the United Kingdom. The BS tested in the current work was collected from the intertidal zone of Cheung Chau Island, Hong Kong, and its main mineral composition is also quartz (Fig. 2b). Although both LBS and BS are quartzitic, the BS particles are more angular than those of LBS by visual observation. The CS is a biogenic (skeletal) sand which is mainly produced by accumulation of the skeletal remains of marine organisms, such as corals, coccoliths, shells and so on (Wang et al. 2017; Zhou et al. 2020; Shen et al. 2021). The CS examined was collected from a reef island in the South China Sea. Its mineral composition is mainly aragonite and calcite, and the calcium carbonate content is higher than 90%. Due to the biological nature of CS, its particle morphology is complex with abundant intra-particle pores as shown by the SEM images in Fig. 2c. The CDG soil is the product of granite by in-situ physical or chemical weathering (Lee and Coop 1995; Li et al. 2020) with particles

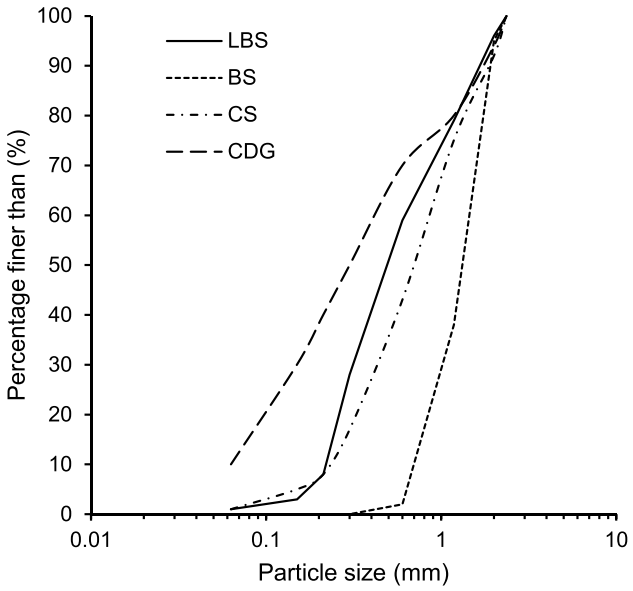

Fig. 1 Particle size distributions of the tested soils

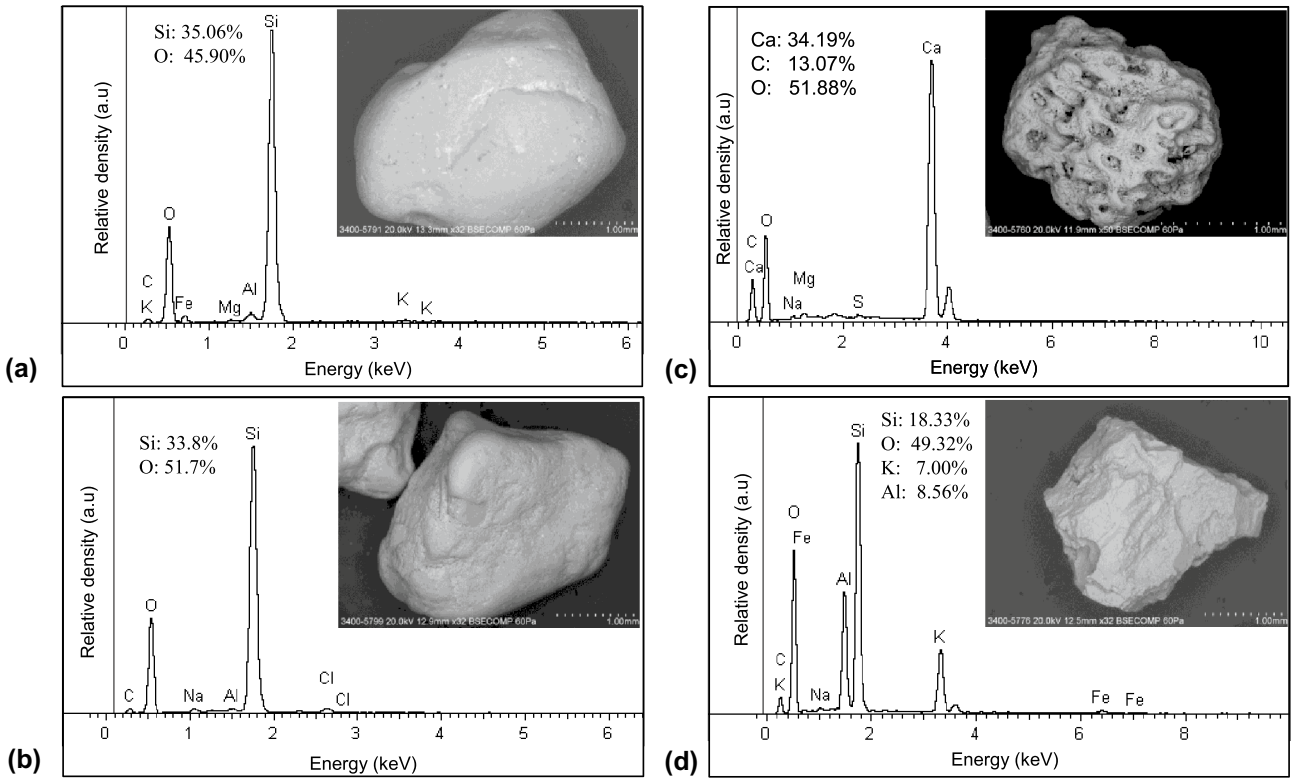

Fig. 2 SEM images and EDX analysis of **a** LBS; **b** BS; **c** CS; **d** CDG

ranging in size from coarse sand to silt. The CDG sand was collected from a construction site at Mt Beacon, Kowloon Tong, Hong Kong. For sandy fraction of CDG, the main components are quartz, plagioclase feldspar and biotite (Sewell 1999; Rocchi and Coop 2016), and its chemical composition comprises 75% silica by weight. The SEM image of CDG shown in Fig. 2d reveals particles with high angularity and rough surfaces.

QicPic particle shape analyser

The particle size and global shape of sand were measured by the QicPic (Sympetac GmBH, Clausthal-Zellerfeld, Germany), which is a dynamic image analysis apparatus for particles between 1 μm and 30 mm. For particles coarser than 0.063 mm, dry dispersion was used to separate sand particles, and its working principle is presented in Fig. 3. A steady particle flow generated by the vibrated feeder could minimize the overlapping of particles during falling. The frame rate of the camera can be as high as 450 Hz, therefore, it only takes a short span of time to measure a large number of particles to obtain statistically representative result. Theoretically, QicPic overcomes the disadvantage of static image analysis that the particle image plane is restricted. WINDOX5 software was used to obtain the particle images and analyse the data.

Optical interferometer

The surface roughness of sand grains was measured by an optical interferometer built on microscope (Microsurf

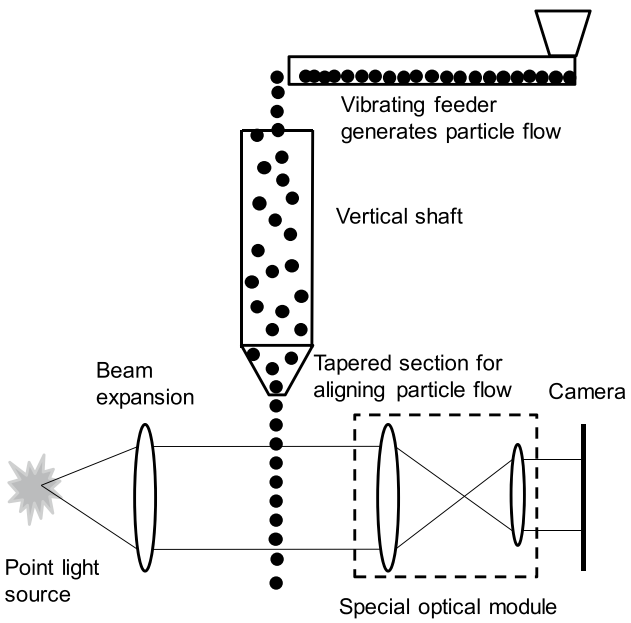

Fig. 3 Working principle of QicPic particle shape analyser

3D, Fogale-Nanotech, Nîmes, France). Compared to other surface roughness measurement apparatuses, i.e., stylus profilometer, atomic force microscope (AFM), and scanning tunnelling microscope (STM), it has the advantages of non-contacting (non-destructive) the examined surfaces, non-conductivity surface applicability, higher measurement speed, and relatively larger size of field of view (140×107 μm^2). The optical interferometer works by splitting the light beam from a selectable light source into two beams that are reflected by a rough surface and a reference mirror, respectively. The two reflected beams combined by a cube are sent through the tube lens to a CCD camera to generate a 3D image. Optical interferometer can perform a surface profile measurement in minutes, but it requires the surfaces to be reflective and not much diffusive. Detailed description can be found in Yao et al. (2019). Its lateral resolution is 0.184 µm, and the vertical resolution can be as high as 10 nm. The apparatus has been successfully adopted to measure the surface roughness of quartz sand (Altuhafi et al. 2013; Nardelli and Coop 2019; Yao et al. 2019).

Particle shape analysis

Particle size and shape

Several particle size characteristics are available in the QicPic system as shown in Fig. 4, in which the Feret diameters are the distances between two parallel lines tangent to the particle outline (d_{Feret_min} and d_{Feret_max} are the maximum and minimum distance, respectively); d_{EQPC} is the diameter of a circle having an equivalent area (the circle indicated by the dash line in Fig. 4) to the particle projection; Aspect ratio (AR) is the ratio between d_{Feret_min} and d_{Feret_max}, varying between 0 and 1; sphericity (S^{QP}) is the ratio of the perimeter of a circle with equivalent area as the particle to the real perimeter of the particle projection, which equals to the circularity defined by Wadell (1932); convexity (C_X) is the ratio between the actual area of the particle and the area of the convex hull, which is similar to how ISO solidity measures the compactness of a particle. Both Cavarretta et al. (2010) and Zheng and Hryciw (2015) compared the sphericity, S^{KS}, used in the reference chart proposed by Krumbein and Sloss (1963) with the computation geometry results of other shape parameters, and claimed that the calculations of S^{KS} are actually based on AR. Sphericity (S^{QP}) used in QicPic system was discovered to be related to both S^{KS} and roundness used in the Krumbein and Sloss (1963)'s reference chart (Cavarretta et al. 2010).

Surface roughness

Many parameters have been proposed to quantify surface roughness. When considering the amplitude of surface roughness, central-line-average roughness (S_a) and root-mean-square roughness (S_q) are widely used. However, surfaces of sand particles are not flat, the finer the particles and the sharper the corners, the greater the surface curvature (Yao et al. 2021) within the same measurement area. In order to remove their effect on the surface roughness quantification, shape motif method built in the FOGALE Viewer 3D software was adopted to separate the whole surface into shape and roughness. The 'motif' method aims to filter the surface profiles between regular and irregular properties related to roughness as illustrated by (Boulanger 1992). After separating, the surface roughness was determined by the flattened root-mean-square roughness, RMS_f, which is only related to the roughness (Boulanger 1992) and calculated by using Eq. 1.

$$RMS_f = \sqrt{\frac{1}{MN}\sum_{i=1}^{M}\sum_{j=1}^{N}\left(h^2(i,j)\right)} \quad (1)$$

where, M, N are the numbers of points along the X, Y directions on a measurement area (578×578 for 106.6×106.6 μm^2); h(i,j) denotes the height of discrete points to the reference plane of the surface. Although Yang et al. (2016) and Li et al. (2021) pointed out that 'motif' method ignored the

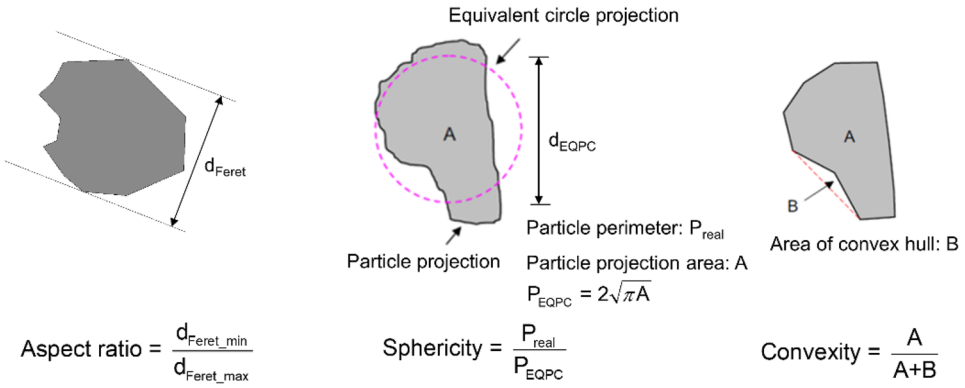

Fig. 4 Definitions of particle sizes and shape used in this study

effect of particle size, its relatively low error and convenience (built in the FOGALE Viewer 3D software) were the main reasons for its application in this study. As reference, Yao et al. (2019) found that the RMS_f of LBS is around 0.45 µm.

Results and discussions

Relationship between particle size and shape

The four types of natural sand were divided into size groups of 0.063–0.15 mm, 0.15–0.212 mm, 0.212–0.3 mm, 0.3–0.425 mm, 0.425–0.6 mm, 0.6–1.18 mm, 1.18–2 mm, and 2–2.36 mm. Altuhafi et al. (2013) claimed that the sample mass required by QicPic to obtain statistically representative particle size and shape depends on its particle size, and Joudi (2008) found that 5 g is an adequate amount for sands between 0.16 and 0.35 mm. Different amounts of BS sand with sizes of 0.6–1.18 mm and 1.18–2.36 mm were firstly tested, to figure out the sample quantity required to acquire statistically representative results for coarser particles. For finer 0.6–1.18 mm BS particles, samples weighed of 5, 8, 10, and 15 g were tested, while for coarser 1.18–2.36 mm particles, 5, 10, 15, and 20 g were measured. The feeder rate of vibration was 6% and the frame rate of the camera was set as 350 Hz. Overlapping phenomenon of particle images was found to be rare from the particle images collected by WINDOX5 software.

Figure 5 presents the particle size distributions (PSD) of BS with different masses, in which the particle size is represented by d_{Feret_min} as it is closest to the sieve data (Altuhafi et al. 2013). Obvious difference was noted in the PSD curves, indicating that 5 g is not enough for coarser particles. The mean values of particle sizes in terms of d_{Feret_min}, d_{Feret_max}, d_{Feret_mean}, and d_{EQPC}, and shape parameters including AR, S^{QP}, and C_X for BS with different masses were summarized in Table 1. When the sample mass is greater than 10 g and 15 g for 0.6–1.18 mm and 1.18–2.36 mm sized particles, the mean values of particle sizes and shape tend to stabilize. In this study, the sample masses used for particle size and shape measurements vary from 3 g for 0.063–0.15 mm to 15 g for 2–2.36 mm size group.

Some binary images of selected particles of the four kinds of sand (1.18–2 mm) with size and shape parameters are shown in Fig. 6. The LBS particles are the most spherical and rounded of all sands by visual observation. Quantitatively, the values of particle shape descriptors of LBS particles are much higher, especially the values of S^{QP} are higher than 0.90. Even though BS is also quartzitic, its sharp and angular edges result in a much lower AR and S^{QP} than the LBS shown in this figure. Among these sand particles, the CS was found to be most irregular, with an AR value of as low as 0.34. The CS is a kind of biogenetic sand that remains the original coral skeleton with sharp edges and corners (Kong and Fonseca 2018), therefore its S^{QP} and AR

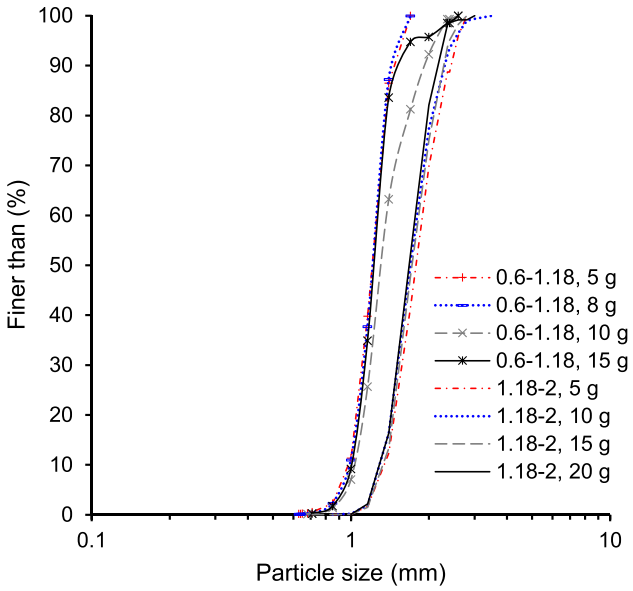

Fig. 5 Sample mass effect on the particle size distribution in terms of d_{Feret_min} of BS with different particle sizes

are much lower. The CDG particles listed in this figure are spheroids, but their corners are much more angular than LBS, with S^{QP} less than 0.90.

However, individual particle or a few particles are not representative of the entire sample. The mean values of particle size and shape for each specimen were summarized in Table 2. They were obtained from the cumulative distributions of d_{Feret_min}, AR, S^{QP}, and C_X by volume, and the resultant values were denoted as d_{50} for d_{Feret_min}, AR_{50} for aspect ratio, $S^{QP}{}_{50}$ for sphericity, and C_{X50} for convexity. In Altuhafi et al. (2013), the AR_{50}, $S^{QP}{}_{50}$, and C_{X50} of LBS with size of 0.7 mm measured by QicPic are 0.74, 0.89, 0.96, respectively. Wei et al. (2020) quantified the particle shape of carbonate gravel with size of 10–20 mm by $PartAn^{3D}$, and the AR_{50}, $S^{QP}{}_{50}$, and C_{X50} are around 0.60, 0.86, and 0.95, respectively. For CDG particles coarser than 0.063 mm, the AR_{50} and $S^{QP}{}_{50}$ are 0.75 and 0.83 in Rocchi and Coop (2015). The sand particle shape results obtained in this study are consistent with the above studies. From Table 2, it can be found that the AR_{50}, $S^{QP}{}_{50}$, and C_{X50} of LBS are the highest among tested sands, which demonstrates that the LBS particles are most spherical and rounded.

The relationship between particle size and the three shape parameters for each sand is shown in Fig. 7. It is found that the mean values of particle shape of both LBS and BS increase with particle size as plotted in Fig. 7a, b, indicating that the coarser the LBS and BS particles, the more spherical and rounded the particles. The increases in AR_{50} with particle size for LBS and BS were discovered to be most significant, from 0.729 to 0.800, and 0.712 to 0.749, respectively. The LBS is a kind of fluvial deposit, the streams characteristically

Table 1 Mean values of particle size and shape of beach sand with different masses

Particle size (mm)	Mass (g)	Mean value						
		d_{EQPC} (mm)	d_{Feret_min} (mm)	d_{Feret_max} (mm)	d_{Feret_mean} (mm)	Sphericity	Aspect ratio	Convexity
0.6–1.18	5	1.39	1.21	1.88	1.56	0.863	0.712	0.960
	8	1.41	1.22	2.05	1.67	0.867	0.709	0.961
	10	1.44	1.22	1.88	1.55	0.862	0.698	0.959
	15	1.42	1.23	1.89	1.55	0.862	0.708	0.959
1.18–2.36	5	2.00	1.79	2.57	2.19	0.870	0.729	0.964
	10	1.90	1.70	2.43	2.06	0.872	0.731	0.966
	15	1.94	1.72	2.45	2.10	0.870	0.738	0.966
	20	1.91	1.72	2.43	2.07	0.873	0.735	0.965

rounded the sand particles with respect to the attrition effect if the size is not finer than 0.05 mm during transportation (Grout 1932). Russell and Taylor (1937) pointed out that within the sand size range, the roundness and sphericity of coarser particles of both beach and river sands are higher. The sands are reduced in size chiefly by fracturing, chipping, and cleavage so that most of them consists of angular blocks with freshly broken surfaces (Zuo et al. 2019). Particles finer than 0.1 mm in diameter could not be rounded in water (Daubrée 1879), so the corners and edges of finer particles are more angular. Compared to LBS, even made up of the same mineralogy, the BS particles are less spherical and rounded. On the one hand, the BS contains a small part of irregular shaped feldspar, and the content of feldspar increases with decreasing particle size. On the other hand, the BS probably experienced much less aqueous (wave) traction transportation distance than the LBS, as it is concluded that any rounding of sand grains by aqueous traction transportation requires travel of many thousands of miles (Edwards 2001), and the effect of wave traction transportation on particle rounding increases with dimension (Twenhofel 1945).

Figure 7c presents the mean values of particle shape descriptors of CS against particle size. The values of the shape parameters of CS were found to be lower than those of LBS and BS with same particle sizes. The CS is mainly formed by the accumulation of the skeletal remains of marine organisms with complex particle morphology, abundant cavities and intra-particle pores (Zhou et al. 2020), therefore its

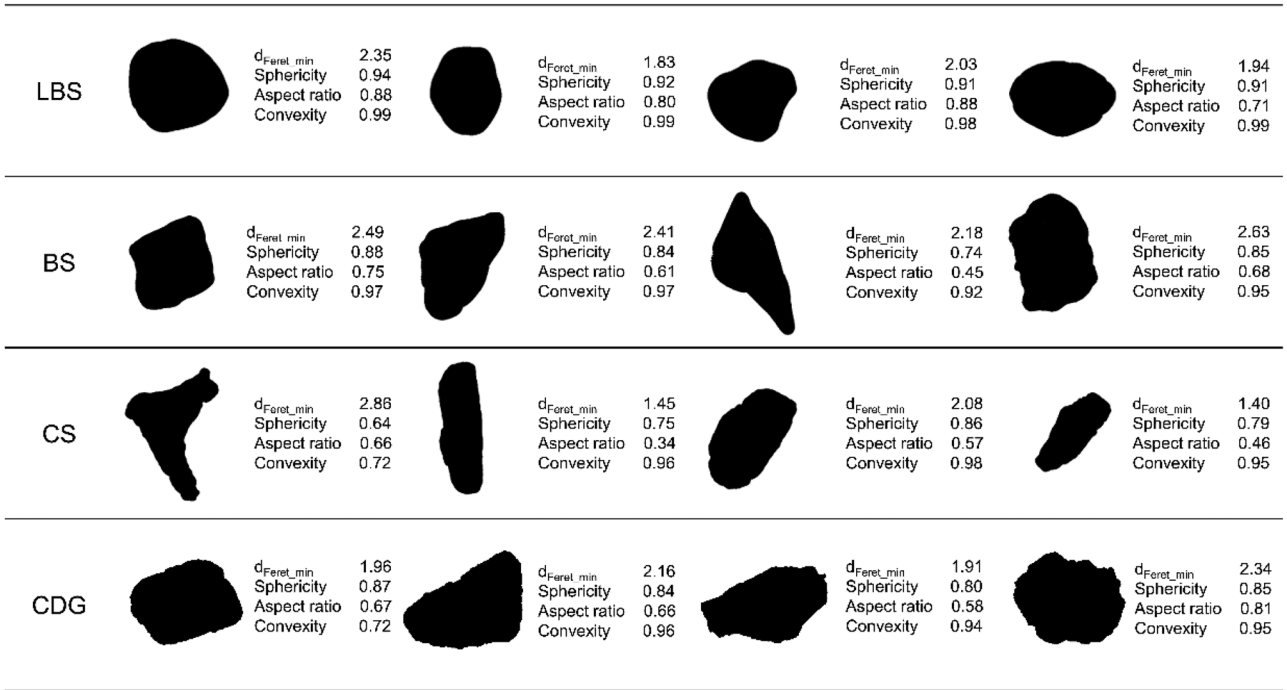

Fig. 6 Binary images of four kinds natural sand with size of 1.18–2.00 mm

Table 2 Summary of particle size and shape of tested sands

Sand type	Particle size (mm)	d_{Feret_min} d_{50} (mm)	Aspect ratio AR_{50}	Sphericity S^{QP}_{50}	Convexity C_{X50}	Quantitative	References	Qualitative	References
LBS	0.15–0.212	0.205	0.729	0.881	0.920	$C_{X50}=0.96$	Altuhafi et al. (2013)	Rounded	Yoshida et al. (2004)
	0.212–0.3	0.288	0.745	0.888	0.938	$S^{QP}_{50}=0.89$			
	0.3–0.425	0.389	0.761	0.893	0.949	$AR_{50}=0.74$			
	0.425–0.6	0.539	0.760	0.894	0.958				
	0.6–1.18	1.099	0.794	0.910	0.975	$d_{50}=0.731$ mm			
	1.18–2	2.000	0.821	0.912	0.984				
	2–2.36	2.529	0.800	0.905	0.976				
BS	0.6–1.18	1.234	0.712	0.863	0.956	NA	NA	NA	NA
	1.18–2	1.789	0.729	0.870	0.964				
	2–5	2.844	0.749	0.868	0.965				
CS	0.063–0.15	0.136	0.720	0.883	0.908	$C_{X50}=0.945$	Yan and Shi (2014)	Angular	Coop et al. (2004)
	0.15–0.212	0.213	0.719	0.872	0.940	$S^{QP}_{50}=0.835$		d = 0.3–0.425 mm	
	0.6–1.18	0.912	0.717	0.850	0.942	$AR_{50}=0.641$			
	1.18–2	1.58	0715	0.849	0.950	d = 1.18–2 mm			
	2–2.36	2.49	0.690	0.828	0.949				
CDG	0.063–0.15	0.141	0.691	0.867	0.902	$C_{X50}=0.85$	Rocchi and Coop (2015)	NA	NA
	0.212–0.3	0.287	0.696	0.848	0.911	$S^{QP}_{50}=0.91$			
	0.6–1.18	1.024	0.703	0.831	0.937	$AR_{50}=0.68$			
	1.18–2	1.829	0.718	0.829	0.942	$d_{50}=1.51$ mm			
	2–2.36	2.456	0.739	0.823	0.941				

particle shape is much more irregular. It is found that both AR_{50} and S^{QP}_{50} decrease (0.720 to 0.690, 0.883 to 0.828) with particle size, which reveals less spherical and rounded shape of coarser particles. Sphericity used in QicPic takes both AR and roundness into consideration. By comparing the binary images of CS particles with size of 2 mm (Fig. 6) and the SEM images of CS with size of 0.15–0.212 mm (Fig. 8a, b), it is found that the CS samples with larger sizes contain more rod-shaped particles having low values of S^{QP} and AR. Hence, both AR_{50} and S^{QP}_{50} for coarser particles are lower. An obvious increase in the C_{X50} (0.908 to 0.949) with particle size might be the result of the reduction of branched-shape particles (Wei et al. 2020).

The relationship between particle shape in terms of AR_{50}, S^{QP}_{50}, and C_{X50} of CDG soil and particle size is presented in Fig. 7d. There are obvious increases in both AR_{50} (from 0.691 to 0.739) and C_{X50} (from 0.902 to 0.941) as the particle size increases, indicating a decrease in angularity with particle size. However, a marked decrease in sphericity, from 0.867 to 0.823, was discovered, meaning less spherical shapes. A similar trend in particle shape and size for completely decomposed volcanic (CDV) rocks was discovered by Zuo et al. (2019). Decomposed soils in tropical regions, CDG and CDV, are produced by chemical and physical weathering of parent rocks. As a result, they are expected to have less rounded and spherical particles than LBS which has been transported before deposition (Chiu and Ng 2014; Zuo et al. 2019). The relatively weaker minerals, such as biotite and feldspar, degrade faster than quartz (Madhusudhan and Baudet 2014). The SEM images of CDG with sizes of 0.063–0.15 mm and 0.15–0.212 mm (see Fig. 8c, d) show that a small number of plate-like particles exist in the samples, which is the crystal of biotite. It might be the reason for the lower values of AR for finer CDG particles. With subsequent weathering, the newly produced finer particles increase in S^{QP} due to the abrasion or collapsing of asperities of coarser particles. For large particles, the concavities might be infilled by fine particles and the overall C_X increases.

Effect of size of field of view on surface roughness

The surface roughness of both glass beads (Cavarretta 2009; Otsubo et al. 2014) and LBS are proved to increase with the size of field view (Yao et al. 2019). As listed in Table 3, the size of field of view used for surface roughness measurement varies from 20×20 μm^2 for LBS (Altuhafi and Baudet 2011) to 140×106 μm^2 for glass beads (Cavarretta et al. 2010). A similar analysis was performed to investigate

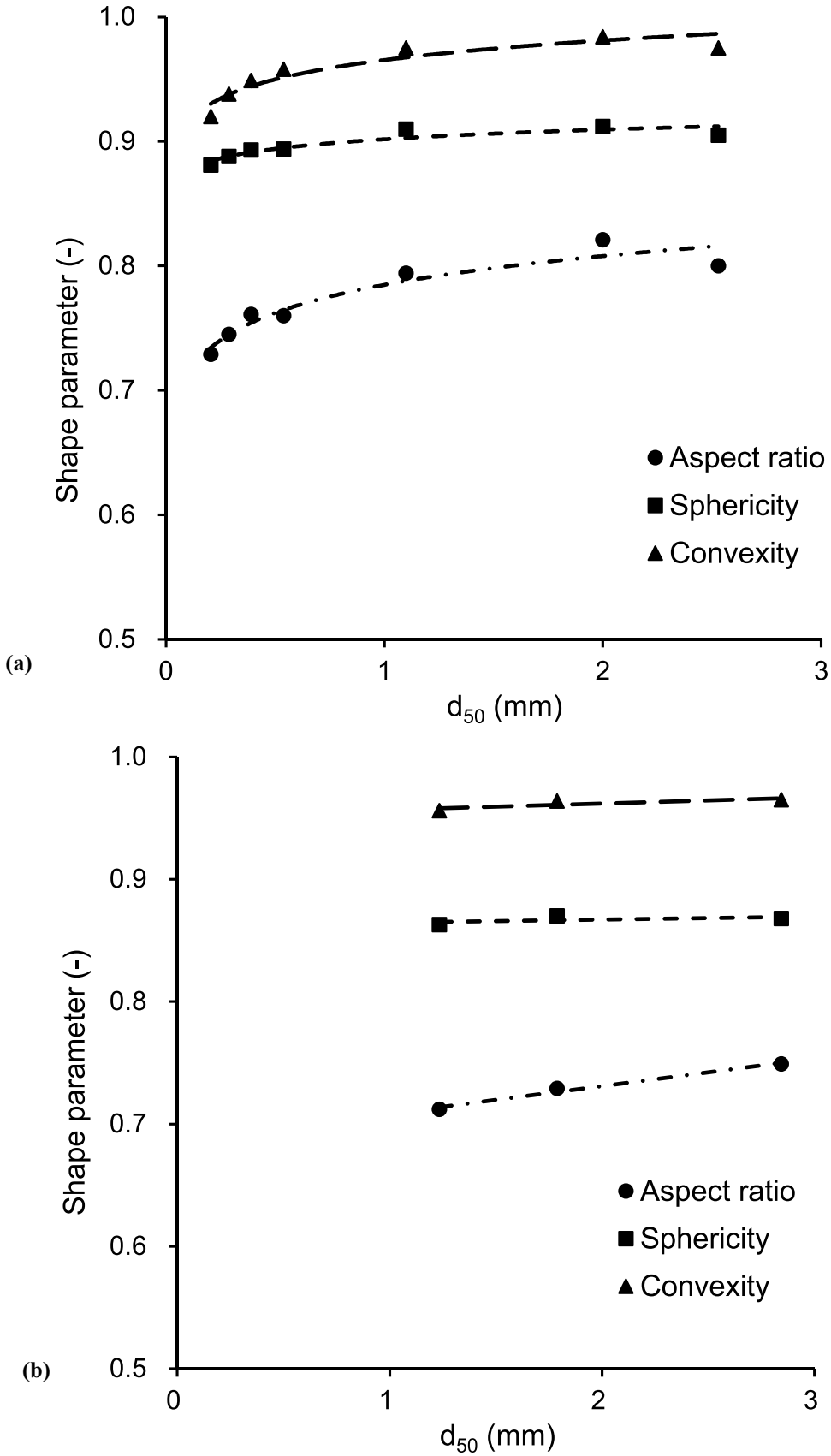

Fig. 7 The relationship between particle size and shape of four kinds of sand: **a** LBS; **b** BS; **c** CS; **d** CDG

Fig. 7 (continued)

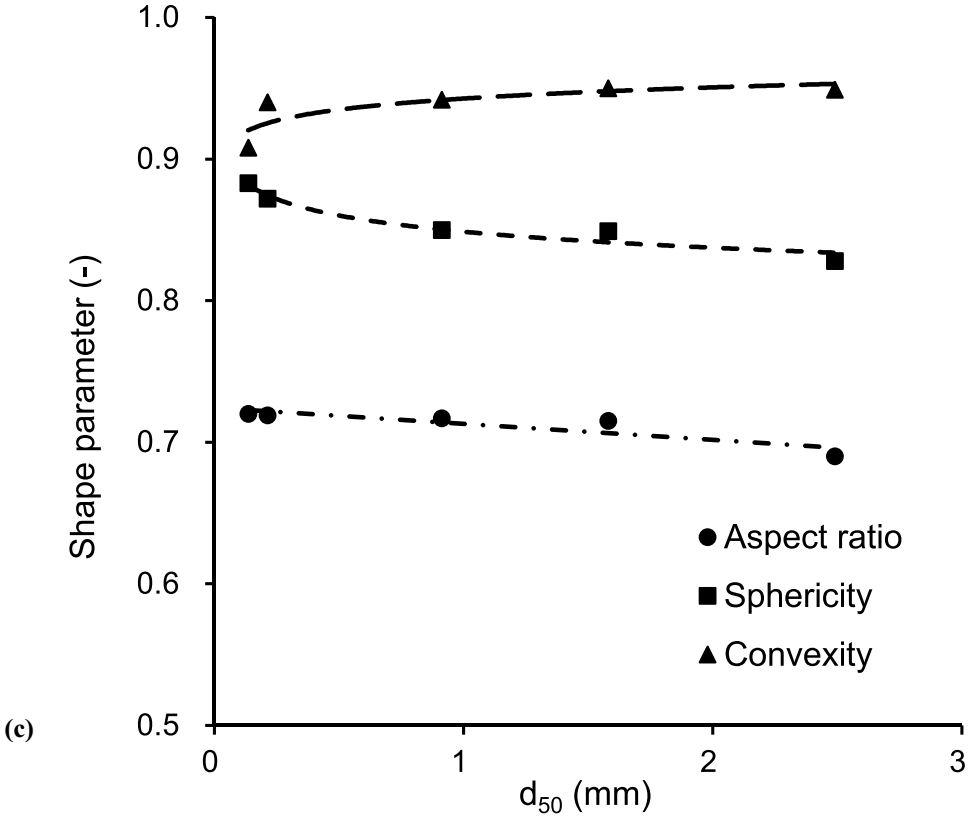

(c)

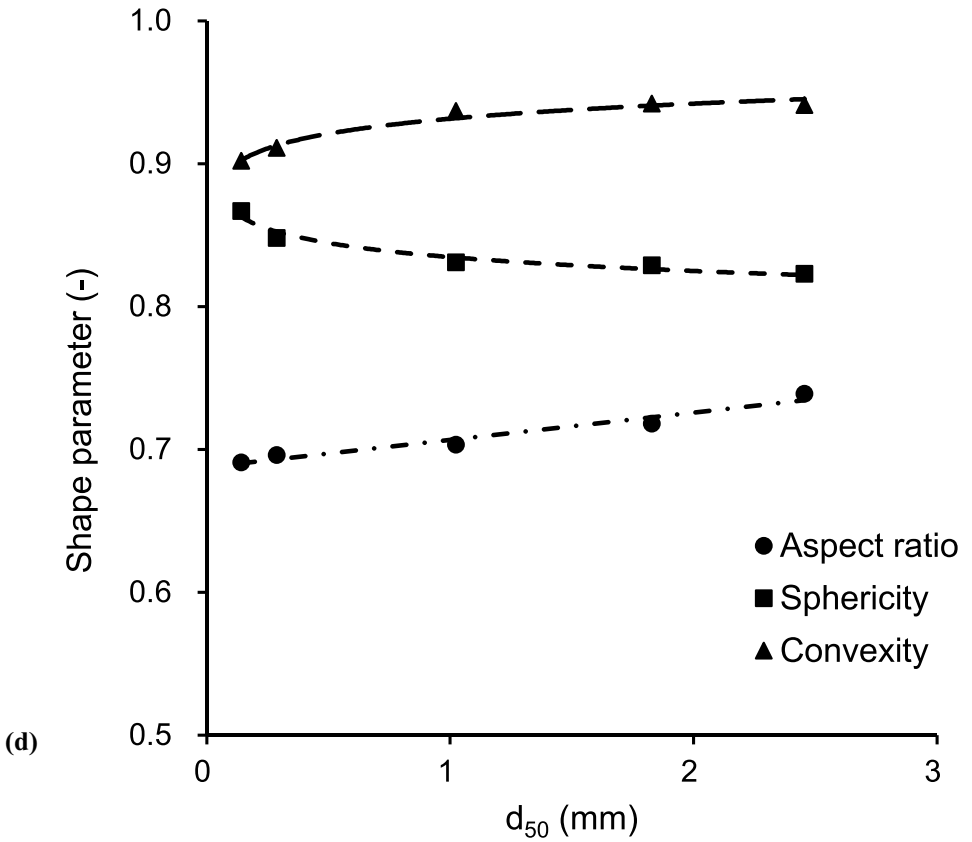

(d)

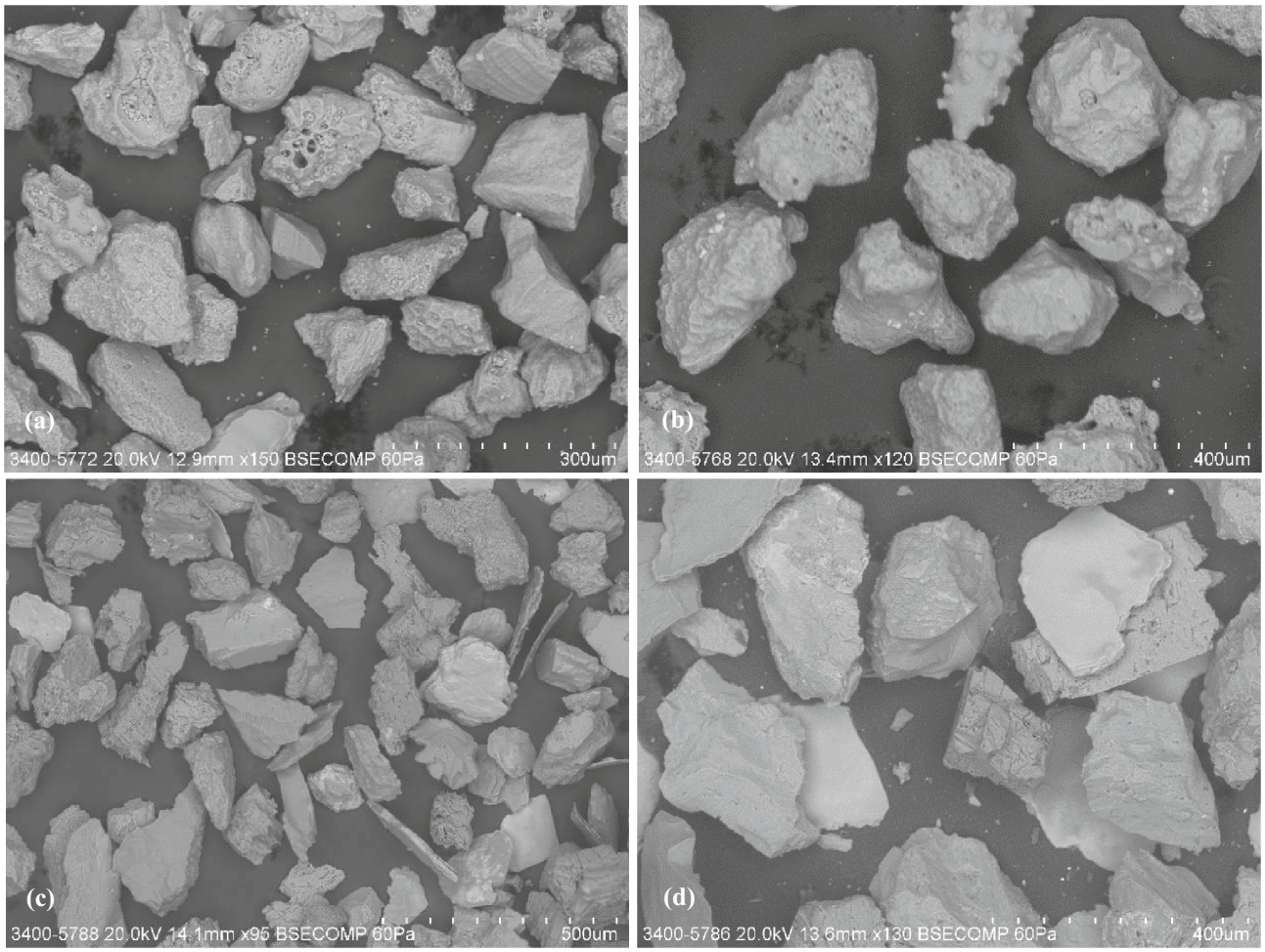

Fig. 8 SEM images of **a** CS of 0.063–0.15 mm; **b** CS of 0.15–0.212 mm; **c** CDG of 0.063–0.15 mm; **d** CDG of 0.15–0.212 mm

the influence of size of field of view on the surface roughness quantification of BS and CS. The surface roughness of CDG particles was not measured due to its unsatisfactory measurement results by optical interferometry, which are caused by the high particle angularity and the relatively low reflectivity of feldspar. The method of using continuously decreasing data set for the calculation of RMS_f is the same as that proposed by Yao et al. (2019). The irregular particle shape and the intra-particle pores of CS particles (Fig. 2c) result in less satisfactory roughness measurement results. In order to minimize the number of invalid pixels within the field of view to guarantee the experimental data accuracy, the maximum areas used for BS and CS were 106.6 × 106.6 μm^2 and 60 × 60 μm^2, respectively.

Figure 9 shows the relationship between the size of field of view and the values of RMS_f for BS and CS particles with different sizes. The X coordinate in this figure is the ratio of the measured field of view area to the minimum area

Table 3 Review of the size of field of view used for surface roughness measurement

Reference	Material	Particle size (mm)	Size of field of view (μm^2)
Alshibli and Alsaleh (2004)	Silica sand	0.22; 0.55; 1.6	Not specified
Cavarretta et al. (2010)	GB	1.0–1.4; 2.4–3.0	106 × 140
Altuhafi and Baudet (2011)	LBS	Not specified	20 × 20
Otsubo et al. (2015)	GB	2.4–2.7	90 × 90
Yang et al. (2016)	LBS	0.60–1.18; 1.18–2; 2–5	106.6 × 106.6
Nardelli et al. (2017)	Eglin sand	1.40–1.55	30 × 30

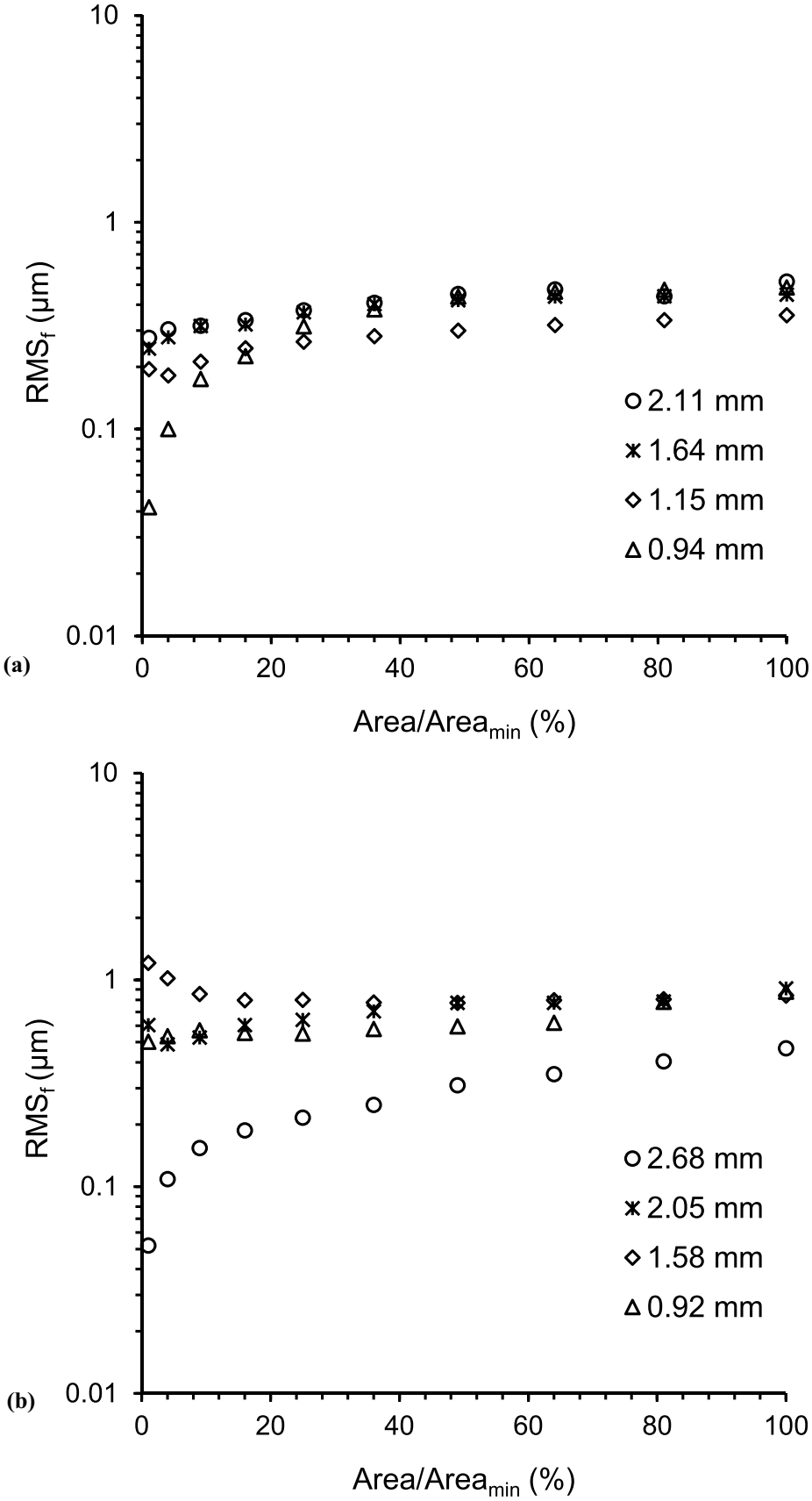

Fig. 9 Relationship between the size of field of view and RMS_f of **a** BS; **b** CS

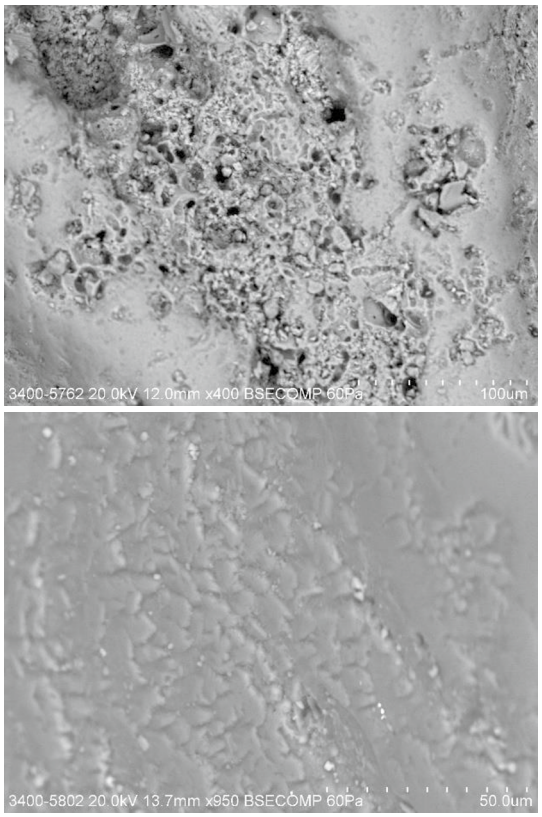

Fig. 10 SEM images of the surface texture of natural sand particles: **a** CS; **b** BS

(10.7 × 10.7 μm^2 for BS, and 6.0 × 6.0 μm^2 for CS), and the numbers in the legend represent the diameters of the tested particles. For each particle, the particle size was carefully measured by a digital micrometer (Mitutoyo IP54) with a repeatability of 1–2 μm at three orthogonal directions. The RMS_f of BS particles was found to increase firstly with the size of field of view and then tend to be stable (Fig. 9a), which is similar with the findings on LBS (Yao et al. 2019). Compared to quartzitic sands, the surfaces of CS particles are much rougher, and the RMS_f presents different trends with increasing size of field of view (Fig. 9b). Figure 10a shows a high magnification SEM image of the surface texture of a CS particle, the microscopic intraparticle pores and the mineral corrosions are unevenly distributed in the testing area. It is different from the surface texture of BS particle as shown in Fig. 10b. Nevertheless, the RMS_f of CS particles with different sizes also tends to be constant over a relatively large measurement area. As a result, using RMS_f obtained from the field of view of 60 × 60 μm^2 to represent the surface roughness of CS and to compare with other types of sand is reasonable.

Effect of particle size on the surface roughness

Due to the difficulty in measuring surface roughness of fine particles by optical interferometry, only particles coarser than 0.8 mm of LBS, BS and CS were tested to study the effect of particle size. Glass beads (GB) with three different sizes were used as references. The test program is listed in Table 4. Thirty particles of each size were randomly chosen, and the surface roughness was measured at the apex in the most stable direction of each particle. The particle size is the average value of the dimensions measured in three orthogonal directions. The size of field of view of LBS,

Table 4 Mean values and standard deviations of RMS_f of tested materials

Material	Particle size (mm)	Number of particles	Field of view (μm^2)	RMS_f (μm)	
				Mean	Standard deviation
LBS	0.86	30	106.6 × 106.6	0.492	0.223
	1.63			0.421	0.202
	2.10			0.466	0.135
	2.53			0.417	0.132
	3.10			0.453	0.133
BS	1.00	30	106.6 × 106.6	0.512	0.105
	1.37			0.488	0.085
	1.76			0.486	0.082
	2.26			0.527	0.110
CS	0.85	30	60 × 60	0.973	0.189
	1.48			0.965	0.210
	1.98			0.803	0.130
	2.59			0.684	0.180
GB	0.80	30	106.6 × 106.6	0.285	0.040
	1.67			0.239	0.024
	2.82			0.223	0.057

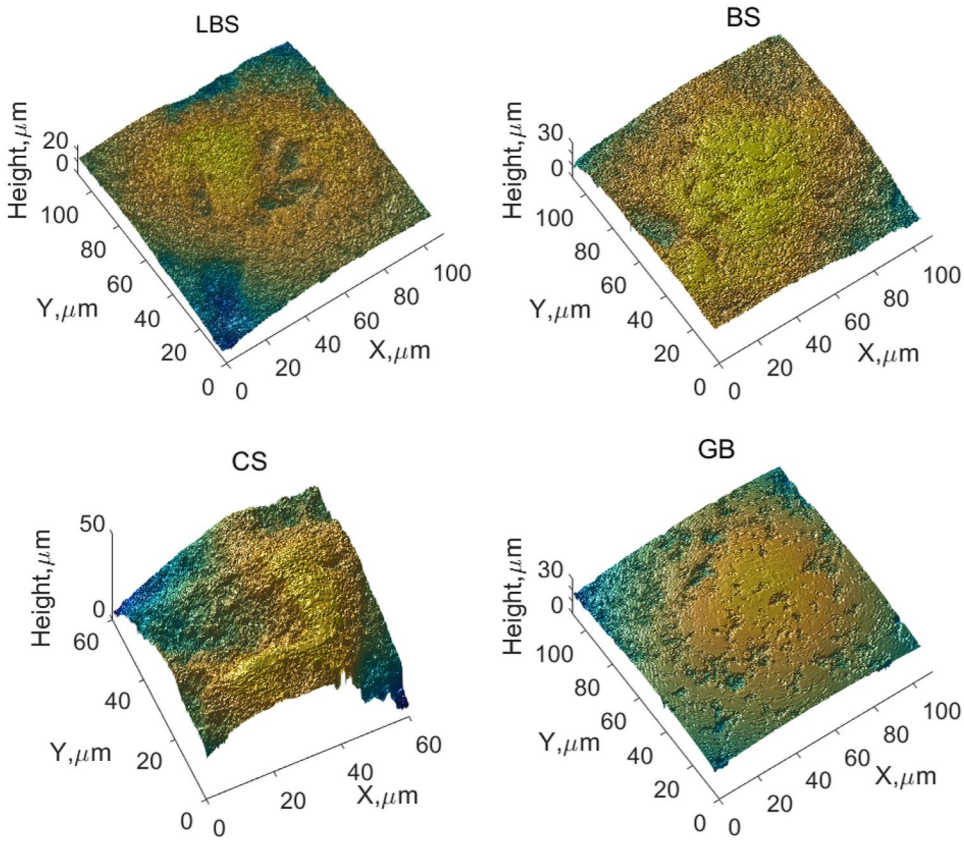

Fig. 11 Surfaces of the tested materials measured by optical interferometry

BS and GB is 106.6×106.6 μm^2, and is 60×60 μm^2 for CS. Figure 11 presents the surface images obtained by optical interferometry of these four granular materials with a diameter of 2 mm. When examined at nanoscale, even the surfaces of GB are not perfectly smooth. The characteristics of the surfaces of those particles vary, and the surface of CS particle is the roughest by visual observation. The mean values and standard deviations of RMS_f for each material are summarized in Table 4.

Figure 12 shows the relationship between particle size and RMS_f in terms of mean values of these four sands, in which the error bars represent the standard deviations of RMS_f. The surface of GB is much smoother than those of natural sand particles, which has the lowest mean value (less than 0.3 μm) and the minimal variation. With increasing particle size, the RMS_f of GB decreases slightly from 0.29 μm to 0.24 μm. The mean values of RMS_f of LBS and BS particles are close (0.4 μm to 0.5 μm), and much higher than that of GB. Both LBS and BS are quartzitic and chemically stable, their surface roughness is assumed to be mainly affected by the physical mechanism during transportation and deposition (Attal and Lavé 2009). Compared to LBS, BS particles might experience less transportation distance and more intensive erosion by seawater, which result in slightly rougher surfaces than those of LBS (Sandeep et al. 2018). The RMS_f of BS decreases first, and increases slightly when the particle size is larger than 1.8 mm. It is hypothesised that the effects of erosion by wave and inter-particle abrasion reach a balance at this size.

Even though the size of field of view used for CS (60×60 μm^2) is about a quarter of that for GB and two quartz sands (106.6×106.6 μm^2), the mean values of RMS_f of CS is the highest. In general, the higher the RMS_f, the rougher the surface. The mineral composition of CS is mainly aragonite and calcite, which can potentially be dissolved by acidified seawater (Muehllehner et al. 2016; Zhong et al. 2022). The intra-particle pores and defects on the CS particle surfaces (Fig. 10a), also might be the reasons for its rougher and more variable surface than that of quartz sand. Particle size plays an important role in the surface roughness of CS. When the particles are finer than 1.5 mm, the mean values of RMS_f decrease slightly, from 0.973 to 0.965, with increasing particle size. For larger particles (> 1.5 mm), a marked reduction of RMS_f (from 0.965 to 0.684) with increasing particle size was discovered. The coarser particle surface is more likely to experience more wave erosion, which may result in the smoother surface.

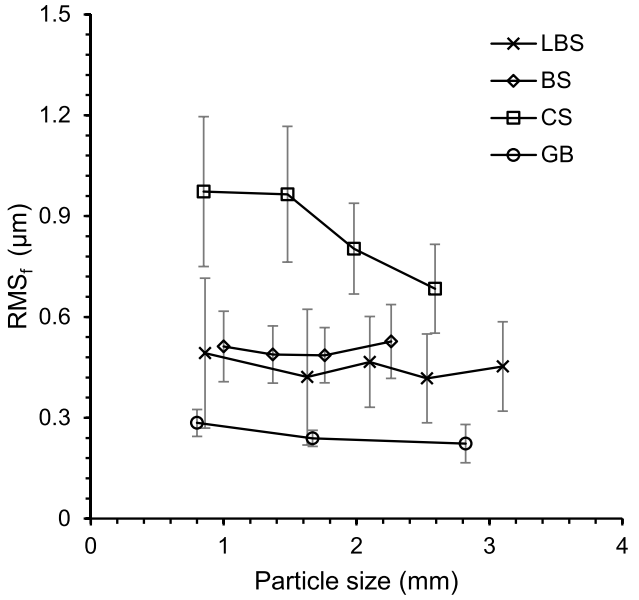

Fig. 12 Relationship between particle size and RMS_f of tested materials

Conclusions

In the current work, the global shape of four types of natural sands was measured by a dynamic particle shape analyser (QicPic), and quantified using three parameters: aspect ratio, sphericity and convexity. The influence of mineralogy, depositional environment, and particle size on particle shape was discussed. The surface roughness of two quartzitic sands and a carbonate sand was successfully measured by optical interferometry and quantitatively characterized, with glass beads tested as references. The main findings are as follows:

1. Both mineralogy and depositional condition have been found to affect markedly the particle shape of natural sand. Among the four sands, the mean values of three shape descriptors of LBS are the highest, indicating the most spherical and rounded shape. Because of the relatively less aqueous traction transportation distance, the corners of BS grains are more angular compared to LBS. For LBS and BS, the mean values of aspect ratio, sphericity and convexity increase with increasing particle size. The particle shape of CDG is much less regular than quartz sands. Both aspect ratio and convexity of CDG increase with increasing particle size. However, its sphericity increases with decreasing particle size due to the abrasion or collapsing of asperities of coarser particles under subsequent weathering. The particle shape of CS is the most irregular, as a large number of grains maintain the skeleton of corals with sharp corners. Both AR_{50} and $S^{QP}{}_{50}$ of CS decrease with increasing particle size, indicating the less spherical and rounded shapes.
2. The size of field of view plays an important role in the surface roughness quantification of natural sands. Although RMS_f of BS and CS with different particle sizes shows different trends with increasing size of field of view, they all tend to be stable at larger sizes. Even though the surface of GB is not perfectly smooth when examined at nanoscale, it is still much smoother than natural sand grains. The mean values of RMS_f of BS is slightly higher than LBS, indicating rougher surfaces. The surface of CS particles is the roughest and the most variable, and the finer the CS particles, the rougher the surfaces.

Funding The authors acknowledge the financial support provided by the National Natural Science Foundation of China (42177154, 42102327, 41402279), the Natural Science Foundation of Hubei Province (2022CFB422), and the Open Fund of Key Laboratory of Special Environment Road Engineering of Hunan Province, Changsha University of Science & Technology (kfj220503).

Data availability The data that support the findings of this study are available from the corresponding author upon reasonable request.

Declarations

Conflicts of interest The authors have no conflicts of interest to declare.

References

Alshibli KA, Alsaleh MI (2004) Characterizing surface roughness and shape of sands using digital microscopy. J Comput Civ Eng 18(1):36–45

Altuhafi F, Baudet BA (2011) A hypothesis on the relative roles of crushing and abrasion in the mechanical genesis of a glacial sediment. Eng Geol 120(1–4):1–9

Altuhafi F, O'Sullivan C, Cavarretta I (2013) Analysis of an image-based method to quantify the size and shape of sand particles. J Geotech Geoenviron Eng 139(8):1290–1307

Attal M, Lavé J (2009) Pebble abrasion during fluvial transport: Experimental results and implications for the evolution of the sediment load along rivers. J Geophys Res Earth Surf 114:F04023

Barrett PJ (1980) The shape of rocks particles, a critical review. Sedimentology 27(3):291–303

Blott SJ, Pye K (2008) Particle shape: a review and new methods of characterization and classification. Sedimentology 55(1):31–63

Boulanger, (1992) An interesting complement to ISO parameters for some functional problems. Int J Mach Tools Manuf 32(1/2):203–209

BS1377–2 (2022) Methods of test for soils for civil engineering purposes - Classification tests and determination of geotechnical properties. British Standards Institution, London, UK

Cavarretta I (2009) The influence of particle characteristics on the engineering behaviour of granular materials. Ph.D. thesis, Department of Civil and Environmental Engineering, Imperial College London, London

Cavarretta I, O'Sullivan C, Coop M (2010) The influence of particle characteristics on the behaviour of coarse grained soils. Géotechnique 60(6):413–423

Chiu C, Ng CWW (2014) Relationships between chemical weathering indices and physical and mechanical properties of decomposed granite. Eng Geol 179:76–89

Cho GC, Dodds J, Santamarina JC (2006) Particle shape effects on packing density, stiffness, and strength: Natural and crushed sands. J Geotech Geoenviron Eng 132(5):591–602
Coop MR, Sorensen KK, Bodas Freitas T, Georgoutsos G (2004) Particle breakage during shearing of a carbonate sand. Géotechnique 54(3):157–163
Daubrée A (1879) Etudes synthetiques de geologie experimentale. Paris
Dyskin AV, Estrin Y, Kanel-Belov AJ, Pasternak E (2001) Toughening by fragmentation–How topology helps. Adv Eng Mater 3(1):885–888
Edwards AC (2001) Grain size and sorting in modern beach sands. J Coastal Res 17(1):38–52
Grout F (1932) Petrography and petrology. McGraw-Hill Book Co, New York
Joudi A (2008) A reassessment of standard laboratory sands. MSc. Dissertation, Imperial College London, London
Kong D, Fonseca J (2018) Quantification of the morphology of shelly carbonate sands using 3D images. Géotechnique 68(3):249–261
Krumbein WC, Sloss LL (1963) Stratigraphy and sedimentation. Freeman, San Francisco
Lee I, Coop MR (1995) The intrinsic behavior of a decomposed granite soil. Géotechnique 45(1):117–130
Li Q, Kim KS (2008) Micromechanics of friction: effects of nanometre-scale roughness. Proc Royal Soc Math Phys Eng Sci 464(2093):1319–1343
Li W, Coop MR (2019) Mechanical behaviour of Panzhihua iron tailings. Can Geotech J 56(3):420–435
Li W, Coop MR, Senetakis K, Schnaid F (2018) The mechanics of a silt-sized gold tailing. Eng Geol 241:97–108
Li W, Kwok CY, Senetakis K (2020) Effects of inclusion of granulated rubber tires on the mechanical behaviour of a compressive sand. Can Geotech J 57(5):763–769
Li Y, Otsubo M, Kuwano R, Nadimi S (2021) Quantitative evaluation of surface roughness for granular materials using Gaussian filter method. Powder Technol 388:251–260
Madhusudhan BN, Baudet BA (2014) Influence of reconstitution method on the behaviour of completely decomposed granite. Géotechnique 64(7):540–550
Mitchell JK, Soga K (2005) Fundamenatals of Soil Behaviour. John Wiley & Sons, Hoboken, New Jersey
Muehllehner N, Langdon C, Venti A et al (2016) Dynamics of carbonate chemistry, production, and calcification of the Florida Reef Tract (2009–2010): Evidence for seasonal dissolution. Global Biogeochem Cycles 30(5):661–688
Nardelli V, Coop MR (2019) The experimental contact behaviour of natural sands: normal and tangential loading. Géotechnique 69(8):672–686
Nardelli V, Coop MR, Andrade JE, Paccagnella F (2017) An experimental investigation of the micromechanics of Eglin sand. Powder Technol 312:166–174
Otsubo M, O'Sullivan C (2018) Experimental and DEM assessment of the stress-dependency of surface roughness effects on shear modulus. Soils Found 58(3):602–614
Otsubo M, O'Sullivan C, Sim WW (2014) A methodology for accurate roughness measurements of soils using optical interferometry. In: Soga K, Kumar K, Biscontin G, Kuo M (eds) Geomechanics from micro to macro, Proceedings IS-Cambridge 2014. UK, London, pp 1117–1122
Otsubo M, O'sullivan C, Sim WW, Ibraim E (2015) Quantitative assessment of the influence of surface roughness on soil stiffness. Géotechnique 65(8):694–700
Rocchi I, Coop MR (2015) The effects of weathering on the physical and mechanical properties of a granitic saprolite. Géotechnique 65(6):482–493
Rocchi I, Coop MR (2016) Mechanisms of compression in well-graded saprolitic soils. Bull Eng Geol Env 75(4):1727–1739
Russell RD, Taylor RE (1937) Roundness and shape of Mississippi River sands. J Geol 45(3):225–267
Sandeep CS, Todisco M, Senetakis K (2017) Tangential contact behavior of a weathered volcanic landslide material from Hong Kong. Soils Found 57:1096–1102
Sandeep CS, He H, Senetakis K (2018) An experimental micromechanical study of sand grain contacts behavior from different geological environments. Eng Geol 246:176–186
Santamarina C, Cascante G (1998) Effect of surface roughness on wave propagation parameters. Géotechnique 48(1):129–136
Sewell RJ (1999) Geochemical atlas of Hong Kong, Geotechnical Engineering Office, Civil Engineering and Development Department, Hong Kong, 110 pp
Shen J, Wang X, Wang X, Yao T, Wei H, Zhu C (2021) Effect and mechanism of fines content on the shear strength of calcareous sand. Bull Eng Geol Env 80(10):7899–7919
Twenhofel W (1945) The rounding of sand grains. J Sediment Res 15(2):59–71
Wadell HA (1932) Volume, shape, and roundness of rock particles. J Geol 40(5):1074–1106
Wang X, Wang X, Jin Z, Meng Q, Zhu C, Wang R (2017) Shear characteristics of calcareous gravelly soil. Bull Eng Geol Env 76(2):561–573
Wei H, Zhao T, Meng Q, Wang X, Zhang B (2020) Quantifying the morphology of calcareous sands by dynamic image analysis. Int J Geomech 20(4):04020020
Witt W, Köhler U, List J (2004) Direct imaging of very fast particles opens the application of powerful (dry) dispersion for size and shape characterisation. Partec
Yan WM, Shi Y (2014) Evolution of grain grading and characteristics in repeatedly reconstituted assemblages subject to one-dimensional compression. Géotechnique Letters 4(3):223–229
Yang HW, Baudet BA, Yao T (2016) Characterization of the surface roughness of sand particles using an advanced fractal approach. Proc Royal Soc A 472(2194):20160524
Yao T, Baudet BA, Lourenço SD (2019) Quantification of the surface roughness of quartz sand using optical interferometry. Meccanica 54(4):741–748
Yao T, Baudet BA, Lourenço SD (2021) Evolution of surface roughness of single sand grains with normal loading. Géotechnique 72(6):543–555
Yao T, Yang HW, Lourenço SD, Baudet BA, Kwok CY (2022) Multiscale particle morphology evolution in rotating drum tests: Role of particle shape and pore fluid. Eng Geol 106669
Yimsiri S, Soga K (2000) Micromechanics-based stress–strain behaviour of soils at small strains. Géotechnique 50(5):559–571
Yoshida S, Johnson HD, Pye K, Dixon RJ (2004) Transgressive changes from tidal estuarine to marine embayment depositional systems: The Lower Cretaceous Woburn Sands of southern England and comparison with Holocene analogs. AAPG Bull 88(10):1433–1460
Zheng J, Hryciw RD (2015) Traditional soil particle sphericity, roundness and surface roughness by computational geometry. Géotechnique 65(6):494–506
Zhong Y, Li Q, Wang R, Yao T (2022) Changes of Physical and Mechanical Properties of Coral Reef Limestone under CO2–Seawater–Rock Interaction. Appl Sci 12(9):4105
Zhou B, Ku Q, Wang H, Wang J (2020) Particle classification and intraparticle pore structure of carbonate sands. Eng Geol 279:105889
Zuo L, Lourenço SD, Baudet BA (2019) Experimental insight into the particle morphology changes associated with landslide movement. Landslides 16(4):787–798